Progress In Electromagnetics Research Letters, Vol. 14, 127–132, 2010

COMPLEMENTARY SPLIT RING RESONATORS OF LARGE STOP BANDWIDTH

S. N. Khan †

Department of Physics
COMSATS Institute of information Technology
Defense Road Off Raiwind Road Lahore, Pakistan

X. G. Liu, L. X. Shao, and Y. Wang

School of Electronic Information Engineering
Soochow University
Suzhou, Jiangsu 215006, China

Abstract—Novel complementary split ring resonator (CSRR) is introduced to increase the stop bandwidth. Despite of their exotic behavior due to negative permittivity, their performance is limited by their stop bandwidth. The orientation of CSRR etched on the ground has strong coupling that can be altered for the increased stop bandwidth. The proposed design has measured stop band from $4 \sim 7.25$ GHz whereas conventional CSRR of same dimension has stop band from $4.1 \sim 5.0$ GHz.

1. INTRODUCTION

The idea of double negative materials proposed by Veselago [1] gained extraordinary research interest after the experimental verification done by Smith [1, 2]. Complementary split ring resonators are the key component to achieve negative dielectric constant (ε). These particles are the negative image of split ring resonators (Babinet's principle) [3] and an axial time varying electric field is necessary to excite the rings that create an effective negative ε medium and inhibit signal propagation at resonance.

Corresponding author: S. N. Khan (snkhan@kth.se).
† Also with School of Electronic Information Engineering, Soochow University, Suzhou, Jiangsu 215006, China.

Artificial transmission lines based on CSRR are useful for the implementation in microwave devices due to their peculiar nature and small size. Artificial transmission lines offer improved performance, novel functionalities and miniaturization [4–6]. These structures have recently been implemented in several microwave devices [7–10]. Although the bandwidth of CSRR is greater than SRR, it is small enough for practical applications. Some studies were conducted keeping in view the bandwidth/size requirements [11–13].

Instead of adjusting the shape of CSRR units, larger stop bandwidth can be achieved by changing the orientation of adjacent CSRR units. The orientation of the CSRR units relative to microstrip line has strong coupling and different orientation can be combined to increase the stop bandwidth.

2. DESIGN AND SIMULATION

The design is implemented on a microstrip transmission line of FR-4 substrate ($\varepsilon = 4.7$) and schematics are elaborated in Fig. 1. The design consists of a microstrip line of width 1.75 mm (dark gray color in Fig. 1) on one side of the substrate while the CSRR are etched on the ground plane on the other side. The size of the proposed design is $50 \times 14\,\text{mm}^2$ and the metal thickness is 0.035 mm.

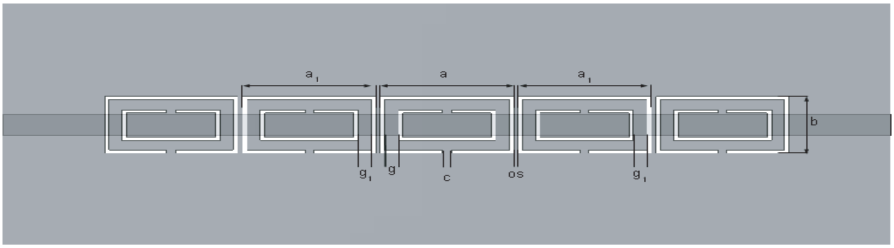

Figure 1. Schematics of the CSRR structures etched on the ground plane. The variables a_1 and g_1 are for design D-III, where the adjacent CSRR units are of different size.

Three different designs named D-I, D-II and D-III will be discussed in this paper. The values of a, c and g are first selected to get stopband for a particular frequency of operation (D-I), which then further exploited by changing the orientation of adjacent CSRR particles to obtain broad stopband (D-II). For the design D-III, CSRR unit of dimension a_1 and g_1 are selected such that the stop band of these CSRR add up with the stop band of CSRR (D-II), to give maximum stop bandwidth. The optimized parametric values from numerical simulation shown in Fig. 1 are listed in Table 1.

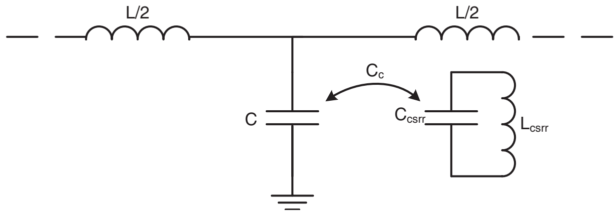

Figure 2. Equivalent circuit model of basic CSRR-loaded microstrip line.

Table 1. Schematic design variable details.

Variable (mm)	c	o_s	a	a_1	b	g	g_1
D-I and D-II	0.5	0.2	6.0	—	3.5	0.6	—
D-III	0.5	0.2	6.0	5.0	3.5	0.6	0.7

The increase in the stop bandwidth due to different orientation of adjacent CSRR particles on the basis of equivalent circuit models shown in Fig. 2 is as follows [14]. The host line is modeled as L and C (per unit inductance and capacitance of host microstrip transmission line). Similarly, CSRR is modeled as resonant structure of L_{csrr} and C_{csrr}. The CSRR are coupled to host transmission line through C_c. It is obvious that the coupling between host line and CSRR (i.e., C_c) varies for different orientations of CSRR; so the stop bandwidth at different frequency is achieved. That eventually adds up and provides larger stop bandwidth compared to conventional design.

The simulation results of conventional CSRR (D-I) and proposed design (D-II) is presented in Fig. 3. As shown in Fig. 3(b), the orientation of adjacent CSRR units in design D-II, are opposite to each other. Based on the simulated results, it is obvious that the D-II provides much better reflection characteristics and larger bandwidth than the conventional design. The stop bandwidth can be further increased by using CSRR units with different size, resulting in signal rejection at different frequencies [9]. In D-III, the adjacent CSRR units not only have opposite orientation but also have different size. The simulated S-parameters for D-III is presented in Fig. 3(c).

3. RESULTS AND DISCUSSION

The comparison between the measured results of D-II and D-III are presented in Fig. 4. The stop bandwidth of D-II ranges $4.18 \sim 6.32$ GHz and $4 \sim 7.25$ GHz for D-III. It is clear that the stop bandwidth of the proposed designs are much greater than the conventional CSRR (4.1 ∼ 5.0 GHz). The measured results slightly shifted to higher frequency than the simulated results but in general follow the simulated pattern. In addition, the measured result shows some ripple better at low frequency which is probably due to lossy FR-4 substrate and fabrication tolerances. Finally, the ideal lossless conditions were used during simulation. The current distribution in Fig. 5, shows that different orientation of CSRR units leads to strong coupling at different

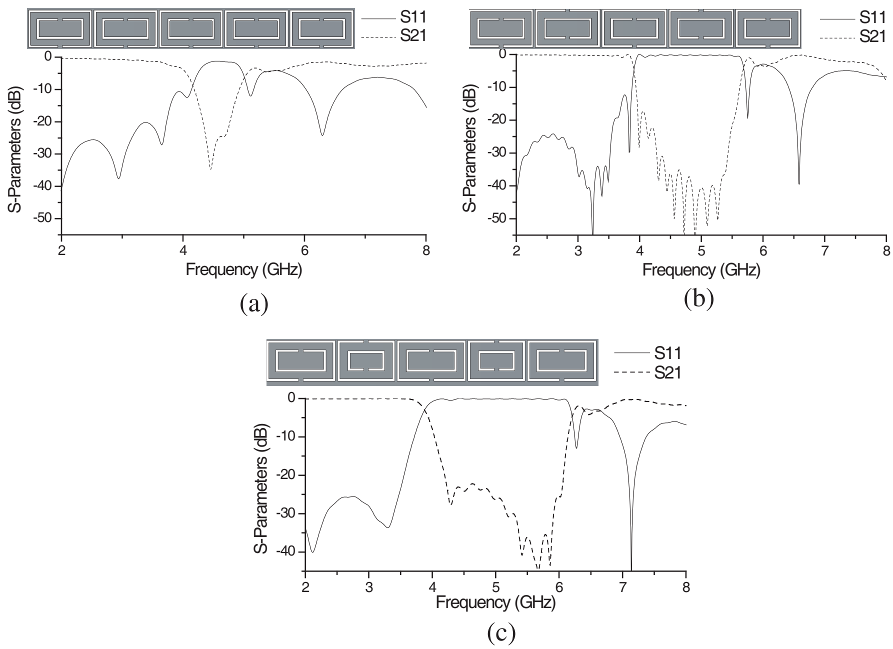

Figure 3. Simulated S-parameters of designs D-I (a), D-II (b) and D-III (c).

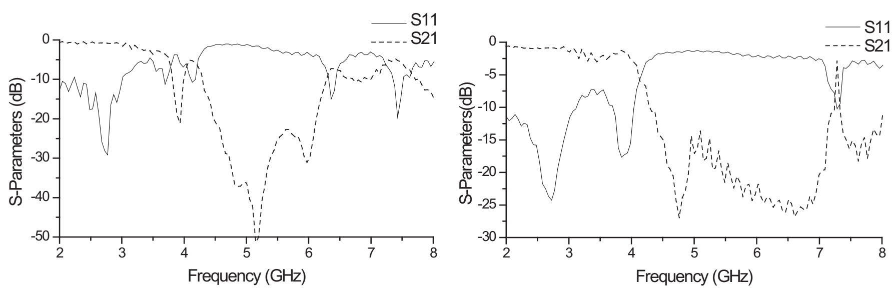

Figure 4. Measured S-parameters of fabricated prototypes, D-II on left and D-III on right side.

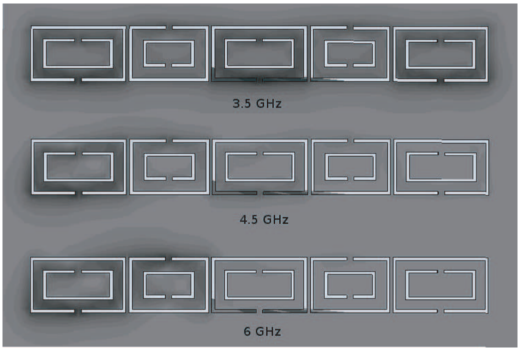

Figure 5. Simulated surface current distribution at different frequencies of D-III.

frequencies. Hence, increased stop bandwidth can be achieved by adjusting both the orientation and the size of CSRR units accordingly. The surface current distribution at 3.5 GHz (pass band) is all over the CSRR in Fig. 4, while the average surface current distribution of D-III at 4.5 and 6 GHz (within stop band) is concentrated around first two CSRR units.

4. CONCLUSION

A new technique for improved stop bandwidth performance is introduced in this paper. The design is suitable for wideband applications. Better results can be obtained by using substrate of superior quality. The design can be further analyzed for SRR where the stop band is even smaller.

REFERENCES

1. Veselago, V. G., "The electrodynamics of substances with simultaneously negative values of ε and μ," *Sov. Phys. Usp.*, Vol. 10, 509–514, 1968.
2. Smith, D. R., W. J. Padilla, D. C. Vier, S. C. Nemat Nasser, and S. Schultz, "Composite medium with simultaneously negative permeability and permittivity," *Phys. Rev. Lett.*, Vol. 84, 4184–4187, 2000.
3. Falcone, F., T. Lopetegi, J. D. Baena, R. Marque's, F. Martín, and M. Sorolla, "Effective negative-epsilon stop-band microstrip lines based on complementary split ring resonators," *IEEE Microwave Wireless Compon. Lett.*, Vol. 14, 280–282, 2004.

4. Khan, S. N., Q. L. Zhang, and S. He, "Left handed microstrip transmission line loaded with combination of split ring resonator and complementary-SRR," *Journal of Electromagnetic Waves and Applications*, Vol. 22, 1857–1863, 2008.
5. Zhang, Q., S. N. Khan, and S. He, "Realization of left handedness through CSRRs and SRRs in microstrip line," *Microwave and Optical Technology Letters*, Vol. 51, No. 3, 757–760, March 2009.
6. Georgieva, A. R., "Investigation of a left-handed microstrip line," *Microwave Review*, 41–44, November 2006.
7. Bahrami, H., M. Hakkak, and A. Pirhadi, "Analysis and design of highly compact bandpass waveguide filter utilizing complementary split ring resonators," *Progress In Electromagnetics Research*, PIER 80, 107–122, 2008.
8. Fu, S. and C. Tong, "A novel CSRR-based defected ground structure with dual-bandgap characteristics," *Microwave and Optical Technology Letters*, Vol. 51, No. 12, 2908–2910, December 2009.
9. Zhang, J., B. Cui, S. Lin, and X.-W. Sun, "Sharp-rejection low-pass filter with controllable transmission zero using complementary split ring resonators," *Progress In Electromagnetics Research*, PIER 69, 219–226, 2007
10. Afkhami, A. and M. Tayarani, "Spurious response suppression in hairpin filter using CSRR merged in the filter structure," *Progress In Electromagnetics Research C*, Vol. 11, 137–146, 2009.
11. Selga, J., G. Siso, M. Gil, J. Bonache, and G. Martin, "Microwave circuit miniaturization with complementary spiral resonators: Applications to high pass filter and dual band components," *Microwave and Optical Technology Letters*, Vol. 51, No. 11, 2741–2725, November 2009.
12. Darcia, J., F. Aznar, M. Gil, J. Bonache, and F. Marjtin, "Size reduction of SRRs for metamaterial and left handed media design," *PIERS Proceedings*, Vol. 3, 266–269, 2007.
13. Ekmekci, E. and G. Turhan-Sayan, "Comparative investigation of resonance characteristics and electrical size of the double-sided SRR, BC-SRR and conventional SRR type metamaterials for varying substrate parameters," *Progress In Electromagnetics Research B*, Vol. 12, 35–62, 2009.
14. Radonić, V., V. Crojecvić Bengin, and B. Jokanović, *On the Orientation of Split Ring Resonators in Metamaterials Media, Serbian, Nis*, 645–648, September 2007.